



OPEN

Protective effects of gallicocatechin gallate against ultraviolet B induced skin damages in hairless mice

Yue-Yue Sheng¹, Jing Xiang¹, Jian-Liang Lu¹, Jian-Hui Ye¹, Zi-Jiu Chen², Jian-Wen Zhao², Yue-Rong Liang¹✉ & Xin-Qiang Zheng¹✉

Epigallocatechin gallate (EGCG) has the effect to protect skin from ultraviolet B (UVB) induced damages, but it is unstable under ambient conditions, being susceptible to become brown in color. Gallicocatechin gallate (GCG), an epimer counterpart of EGCG, is more stable chemically than EGCG. The potential effects of GCG against UVB-induced skin damages has not been available. The objective of this study was to investigate the protective effects of GCG against UVB-induced skin photodamages. GCG was topically applied on the skin of hairless mice at three dosage levels (LL, 12.5 mg/mL; ML 25 mg/mL; HL, 50 mg/mL), with EGCG and a commercially available baby sunscreen lotion SPF50 PA+++ as control. The mice were then irradiated by UVB (fluence rate 1.7 $\mu\text{mol}/\text{m}^2 \text{ s}$) for 45 min. The treatments were carried out once a day for 6 consecutive days. Skin measurements and histological studies were performed at the end of experiment. The results show that GCG treatments at ML and HL levels inhibited the increase in levels of skin oil and pigmentation induced by UVB irradiation, and improved the skin elasticity and collagen fibers. GCG at ML and HL levels inhibited the formation of melanosomes and aberrations in mitochondria of UVB-irradiated skin in hairless mice. It is concluded that GCG protected skin from UVB-induced photodamages by improving skin elasticity and collagen fibers, and inhibiting aberrations in mitochondria and formation of melanosomes.

Skin is the body's first line of defense and it acts as a shield to protect the body from environmental stress. It consists of epidermis, dermis and the subcutaneous tissue. Ultraviolet B (UVB) is the light with a wavelength 280–320 nm. Although the UVB irradiation is less than 5% of total sunlight radiation, it is very harmful to skin due to high absorption by biomolecules such as DNA and proteins. UVB elicits alterations in the epidermal level of the skin¹ and it causes damages to the skin by generating reactive oxygen species (ROS) which induce mitochondrial aberrations, DNA damage and apoptosis in UVB irradiated skins^{2,3}. Prolonged exposure of the skin to UVB irradiation induced degradation of elastic fibers, resulting in skin laxity, dryness, deep wrinkling and pigmentation^{4,5}. Skin melanocytes can synthesize melanin to protect keratinocytes from UVB irradiation^{6,7}. It is interesting to search for natural sunscreen agents to protect skin from photodamages induced by UVB irradiation.

Catechins are a group of bioactive compounds found in tea leaf and they have attracted much attention due to their physiological activities such as anti-inflammatory, antioxidant and anti-cancer^{8–11}. Epigallocatechin gallate (EGCG) is the most abundant catechins, accounting for more than 50% of the total catechins in fresh tea leaves and unfermented green tea¹². Gallicocatechin gallate (GCG) is the spatial isomer of EGCG¹³. Both EGCG and GCG have strong radical-scavenging activity. In the fresh leaves of cultivated tea plants, there is trace amount of GCG. However, GCG is abundant in dry tea because of epimerization of EGCG induced by heating during tea processing^{13,14}. Recent study revealed that GCG is abundant in some wild tea plants, such as *Camellia ptilophylla* and *Camellia assamica* var. *Kucha*^{15–18}.

EGCG was proved to have protective effects against UVB-induced skin damages¹⁹, but it is susceptible to illumination, oxygen and high temperature, resulting in browning in color, which is undesirable in cosmetic products²⁰. GCG, an epimer counterpart of EGCG, is less susceptible to oxygen, heating and illumination²⁰. GCG showed stronger antioxidant activity than EGCG in certain circumstance²¹. It was reported that GCG has stronger free radical scavenging activity than EGCG at low concentration^{22–24}. However, the protective effect of GCG against UVB-induced skin damages has not been available. This study aims to explore the anti-UVB effect

¹Tea Research Institute, Zhejiang University, Hangzhou 310058, China. ²Qiandaohu Beanti-Health Medical Institute Ltd, Hangzhou 311701, China. ✉email: yrliang@zju.edu.cn; xqzheng@zju.edu.cn

of GCG on skin of hairless mice, so as to provide a useful information for developing sunscreen agents against UVB-induced photodamages or photoaging using GCG as ingredient.

Materials and methods

Reagents and equipment. Medical vaseline was purchased from Zhengmao Petrochemical Co. Ltd (Maoming City, China); EGCG (97% purity) and GCG (98% purity) (Fig. S1) were purchased from Ningbo Simingshan Biological Technology Co. Ltd (Yuyao City, China) and they were mixed with the medical vaseline at designed experimental concentration; Water Baby sunscreen lotion with SPF50 PA+++ (Bayer HealthCare LLC, Whippany, NJ, USA) was used as a positive control.

The major equipment used in the test included Ultraviolet Radiometer (Optical Instrument Factory, Beijing, China), transmission electron microscope (TEM) (Hitachi Model H-7650, Hitachi LTD, Tokyo, Japan); CBS-1800 Skin Analyzer (Wuhan Bose Electronic Co., Ltd, Wuhan, China); AB265-S Electronic Balance [Mettler Toledo (China), Shanghai, China]. The UVB was supplied by UVB lamps (Model BLE-1T158, Spectronics corp., Westbury, NY, USA) which emits UV in the range of 254–320 nm, with a peak at 297 nm.

Experimental animals. Five-week-old BALB/c hairless mice used in this study were purchased from Shanghai Slack Laboratory Animal Co., Ltd (Shanghai, China, No. SCXK (Hu) 2017-0005). The mice were housed under a 12 h light /12 h dark cycle at room temperature. During the experimental period, the mice were free to eat feed and drink water. All the animal experiment procedures were approved by the Laboratory Animal Welfare and Ethics Committee of Zhejiang University (Ethics code ZJU20170077). The experiments were performed in accordance with the criteria of the “Guide for the Care and Use of Laboratory Animals” (NIH publication 86-23, revised 1985) and the ARRIVE guidelines (<https://arriveguidelines.org>).

The purchased hairless mice were acclimated under the above controlled conditions for two weeks and then divided into blank control group (BC, without vaseline, GCG and UVB), negative control group (NC, topically treated with vaseline and then irradiated by UVB), positive control group (PC, topically treated with water baby sunscreen SPF50 PA+++ and then irradiated by UVB), EGCG group [EGCG, treated with EGCG (25 mg/mL) and then irradiated by UVB], low level GCG group [LL, topically treated with GCG (12.5 mg/mL) and then irradiated by UVB], medium level GCG group [ML, topically treated with GCG (25 mg/mL) and then irradiated by UVB], high level GCG group [HL, topically treated with GCG (50 mg/mL) and then irradiated by UVB]. Each group contained 13 male and 13 female hairless mice.

Drug application and UVB irradiation. GCG and EGCG were mixed with vaseline according to the above designed concentrations. The drugs including NC, PC, EGCG and GCG at designed concentration were topically smeared on the skin of the tested hairless mice at a dosage 20 $\mu\text{L}/\text{cm}^2$. At 30 min after the drug application, the hairless mice, except BC group, were irradiated with UVB (fluence rate 1.7 $\mu\text{mol}/\text{m}^2 \text{ s}$) for 45 min. The drug application and UVB irradiation were performed once a day for 6 consecutive days. On the seventh day, skin quality indicators including contents of oil, moisture, pigmentation and collagen fiber, and also skin elasticity were determined using CBS-1800 Skin Analyzer according to its instructions. The skin analyzer collects images of the skin to be detected using a CCD camera equipped with polarizing light and transfers the images through a progressive scan image sensor to the data processor where the levels of oil, moisture, pigmentation, collagen fibers and elasticity are evaluated by comparing them with built-in references in the data bank. The skin analyzer gave the indicators with a measurement unit %, which were used to assess the skin quality based on the values obtained from health skins. Then the tested hairless mice were sacrificed and the skins (1 cm^2) were sampled and fixed for 4 h in 2.5% glutaraldehyde dissolved in phosphate buffer (0.1 mol/L, pH 7.0) for transmission electron microscopy (TEM) observation.

Transmission electron microscopy (TEM). The above fixed skin samples were washed in the phosphate buffer (0.1 mol/L, pH 7.0) for 15 min, and the operation was repeated for three times. The washed samples were fixed in 1% OsO_4 dissolved in phosphate buffer (0.1 mol/L, pH 7.0) for 1.5 h and then washed three times in the phosphate buffer as before. The fixed samples were successively dehydrated in a graded series of ethanol (30%, 50%, 70%, 80%, 90% and 95%) for 15 min at each step, and finally dehydrated by 100% ethanol for 20 min. The dehydrated samples were immersed in pure acetone for 20 min, suspended in a mixture of acetone and Spurr resin (1:1) for 1 h at room temperature, then in mixture of acetone: Spurr resin (1:3) for 3 h, and finally in pure Spurr resin overnight.

The above specimens were placed in 1 mL eppendorf tubes containing Spurr resin and heated at 70 °C for more than 9 h. The specimen was sectioned using LEICA EM UC7 ultramicrotome and the sections were stained by uranyl acetate and alkaline lead citrate for 10 min respectively, and finally observed and photographed on Hitachi Model H-7650 TEM.

Assessment of melanosomes. The melanin content of the specimens was evaluated by counting the number of melanosomes in 10 $\mu\text{m} \times 10 \mu\text{m}$ TEM photographs with a constant magnification ($\times 4000$). Five sections per treatment, with three TEM photographs each section, were counted and evaluated.

Assessment of mitochondrial damage index. Mitochondria damage index was evaluated by semi-quantitative scale under constant magnification ($\times 30,000$) of TEM. The following scale was used: 0, no damage in which the mitochondria were rich in mitochondrial matrix and cristae as in Fig. 1A; 1, minimal damage in which the mitochondria were swollen and the cristae were decreased as in Fig. 1B; 2, moderate damage in which

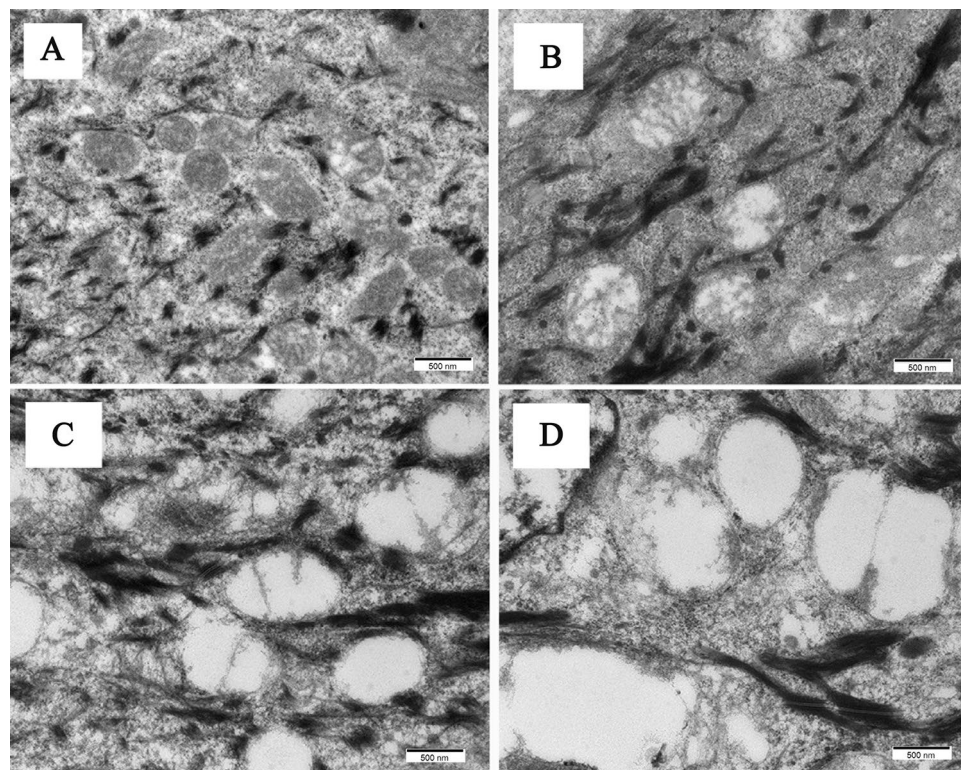


Figure 1. Semiquantitative scale of mitochondria injury degree. (A) scale 0, no damage; (B) scale 1, minimal damage; (C) scale 2, moderate damage; (D) scale 3, heavy damage.

Treatment	Oil	Moisture	Pigmentation	Elasticity	Collagen fibers
BC	4.80 ± 2.49	12.50 ± 3.32	37.00 ± 7.70	38.80 ± 8.93	75.40 ± 2.88
NC	15.68 ± 5.86 [§]	19.17 ± 6.56 [§]	39.40 ± 7.02	36.63 ± 6.45	52.50 ± 8.69 [§]
PC	16.75 ± 3.15 [§]	30.14 ± 5.87 ^{§*}	51.50 ± 6.72 ^{§*}	37.63 ± 6.19	41.86 ± 6.64 ^{§*}
EGCG	5.00 ± 2.28*	32.60 ± 11.91 ^{§*}	46.00 ± 9.03 ^{§*}	63.80 ± 7.01 ^{§*}	77.83 ± 8.30*
LL	16.00 ± 3.22 [§]	19.40 ± 5.68 [§]	40.80 ± 5.54 [§]	35.00 ± 7.14	53.40 ± 8.82 [§]
ML	10.60 ± 4.16 ^{§*}	15.40 ± 5.03*	30.33 ± 4.63 ^{§*}	56.60 ± 15.21 ^{§*}	72.17 ± 10.34*
HL	10.00 ± 4.05 ^{§*}	12.00 ± 6.86*	33.40 ± 1.67 ^{§*}	41.40 ± 3.21*	72.67 ± 3.93*

Table 1. Effect of GCG and EGCG on skin quality indicators after UVB irradiation (%). BC blank control, NC negative control, PC positive control, EGCG EGCG treatment; LL low level GCG treatment, ML medium level GCG treatment, HL high level GCG treatment. [§]Being significantly different from BC at p=0.05. *Being significantly different from NC at p=0.05.

the swollen mitochondria had a few cristae as in Fig. 1C; and 3, heavy damage in which the swollen mitochondria had no cristae. Five sections each treatment were reviewed by three researchers and the mean value was expressed as mitochondrial damage index.

Data analysis. The data were analyzed by software SPSS Statistics V20.0. Mean values of the quantitative data were expressed and the differences between various treatments were tested by T-test at p = 0.05.

Results

Effect of GCG on skin damage induced by UVB. Testing results of skin quality indicators by skin analyzer show that compared to the blank control (BC), UVB irradiation (NC, negative control) induced an increase in levels of skin oil, moisture and pigmentation, accompanying with a decrease in elasticity and collagen fibers in hairless mice skin. Compared to NC and positive control (PC, sunscreen lotion), indicators of skin oil, pigmentation, elasticity and collagen fibers were significantly improved in treatments of EGCG, medium level (ML) and high level (HL) of GCG (Table 1), suggesting that both GCG and EGCG have protective effects against UVB-induced photoaging in hairless mice skin.

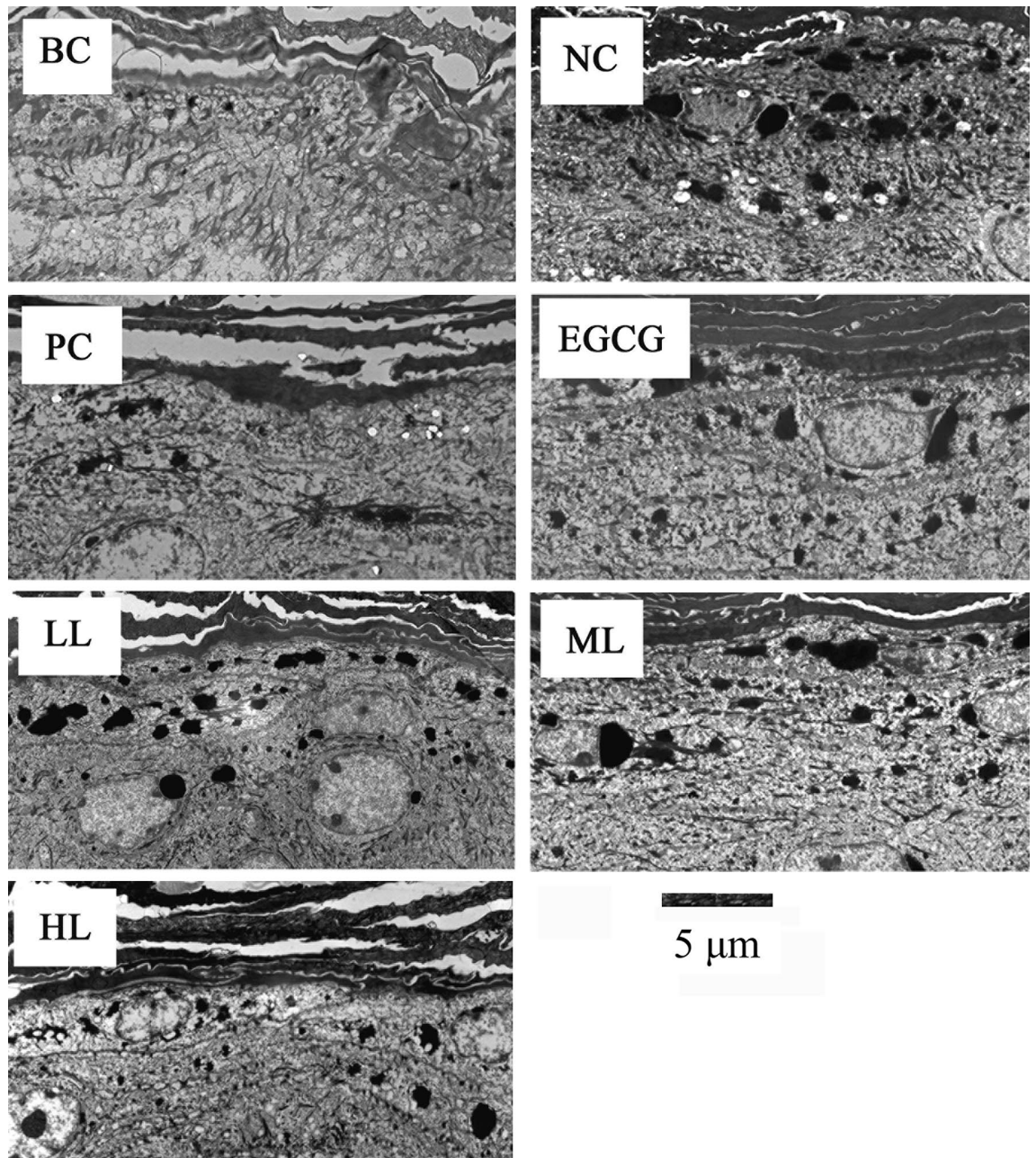


Figure 2. Effects of GCG on UVB-induced melanosome formation in female hairless mice skin. *BC* blank control, *NC* negative control, *PC* positive control, *EGCG* EGCG treatment, *LL* low level GCG treatment, *ML* medium level GCG treatment, *HL* high level GCG treatment, dark dots: melanosomes.

Effect of GCG on melanosome formation induced by UVB. TEM observation and quantitative study show that a few melanosomes were observed in BC both female and male mice and the melanosomes were significantly increased by UVB irradiation in NC (Figs. 2 and 3, Table 2). However, the melanosomes were significantly less in PC and the treatments of EGCG and GCG (LL, ML, HL) in both female and male mice skins, compared to NC (Figs. 2 and 3, Table 2), which were consistent with the pigmentation results in Table 1. These indicate that UVB irradiation stimulated melanosome formation in hairless mice skin, and sunscreen lotion, EGCG and GCG had suppressive effects on UVB-induced melanosome formation.

Effects of GCG on UVB-induced mitochondrial damage. The UVB-irradiation induced changes in mitochondrial structure of skin cells in both female and male mice (Figs. 4 and 5, BC, NC). Before UVB-irradiation, the mitochondria were rich in mitochondrial matrix and cristae (Figs. 4 and 5, BC). The mitochondrial matrix and cristae were markedly reduced in mitochondria of NC. Like PC and EGCG, mitochondria in treatments of ML and HL of GCG contained more mitochondrial matrix and cristae than NC. However, LL had little effects on the reduction of mitochondrial matrix and cristae induced by UVB-irradiation (Figs. 4 and 5, Table 3).

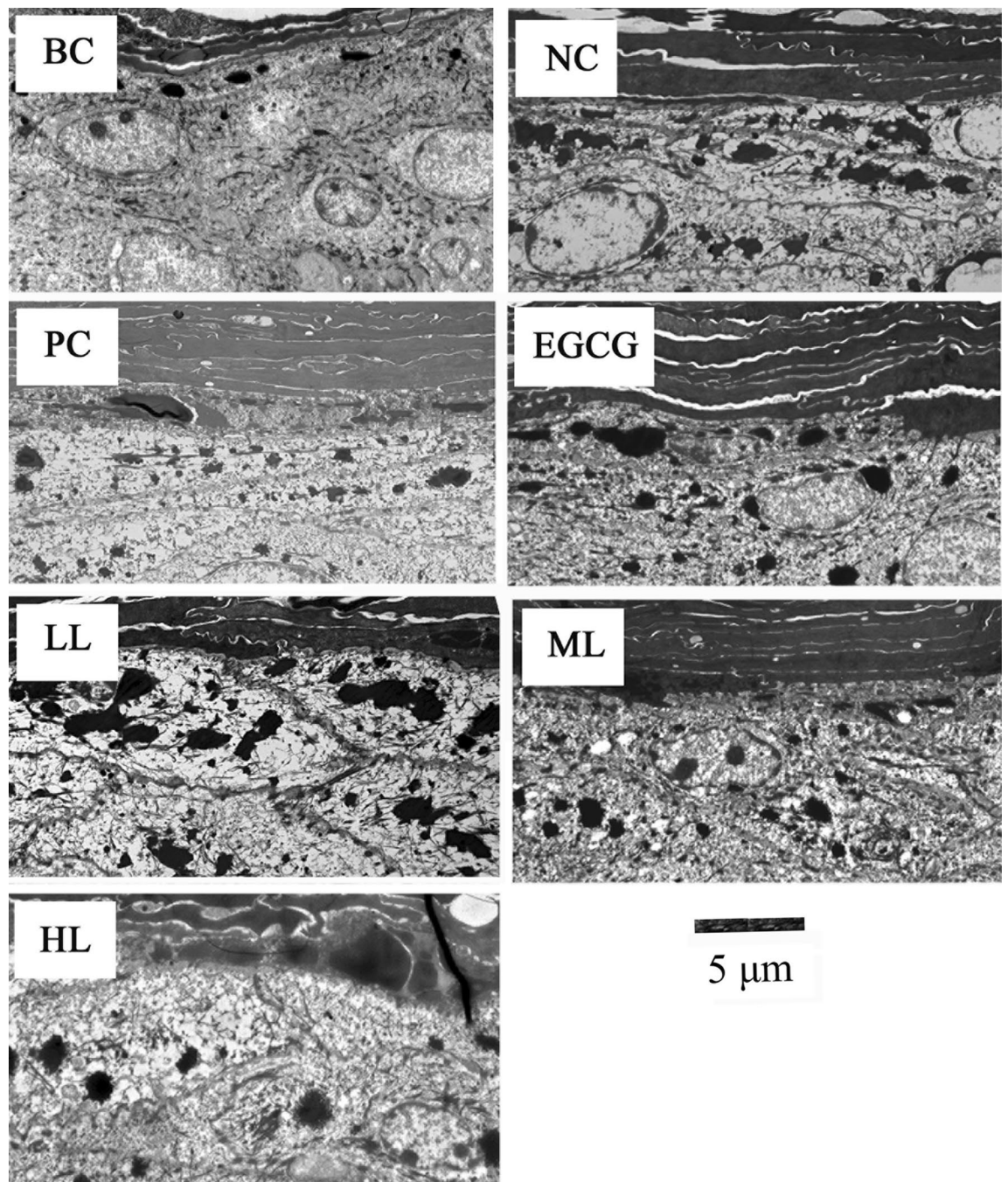


Figure 3. Effects of GCG on UVB-induced melanosome formation in male hairless mice skin. *BC* blank control, *NC* negative control, *PC* positive control, *EGCG* EGCG treatment, *LL* low level GCG treatment, *ML* medium level GCG treatment, *HL* high level GCG treatment, dark dots: melanosomes.

Treatment	BC	NC	PC	EGCG	LL	ML	HL
Melanosomes							
Male	2.73*	15.33 [§]	6.27 ^{§*}	8.53 ^{§*}	14.93 [§]	8.60 ^{§*}	7.27 ^{§*}
Female	3.53*	15.13 [§]	6.27 ^{§*}	7.80 ^{§*}	15.07 [§]	8.47 ^{§*}	7.87 ^{§*}

Table 2. Effect of various treatments on UVB-induced formation of melanosomes. [§]Being significantly different from BC at $p < 0.05$. *Being significantly different from NC at $p < 0.05$.

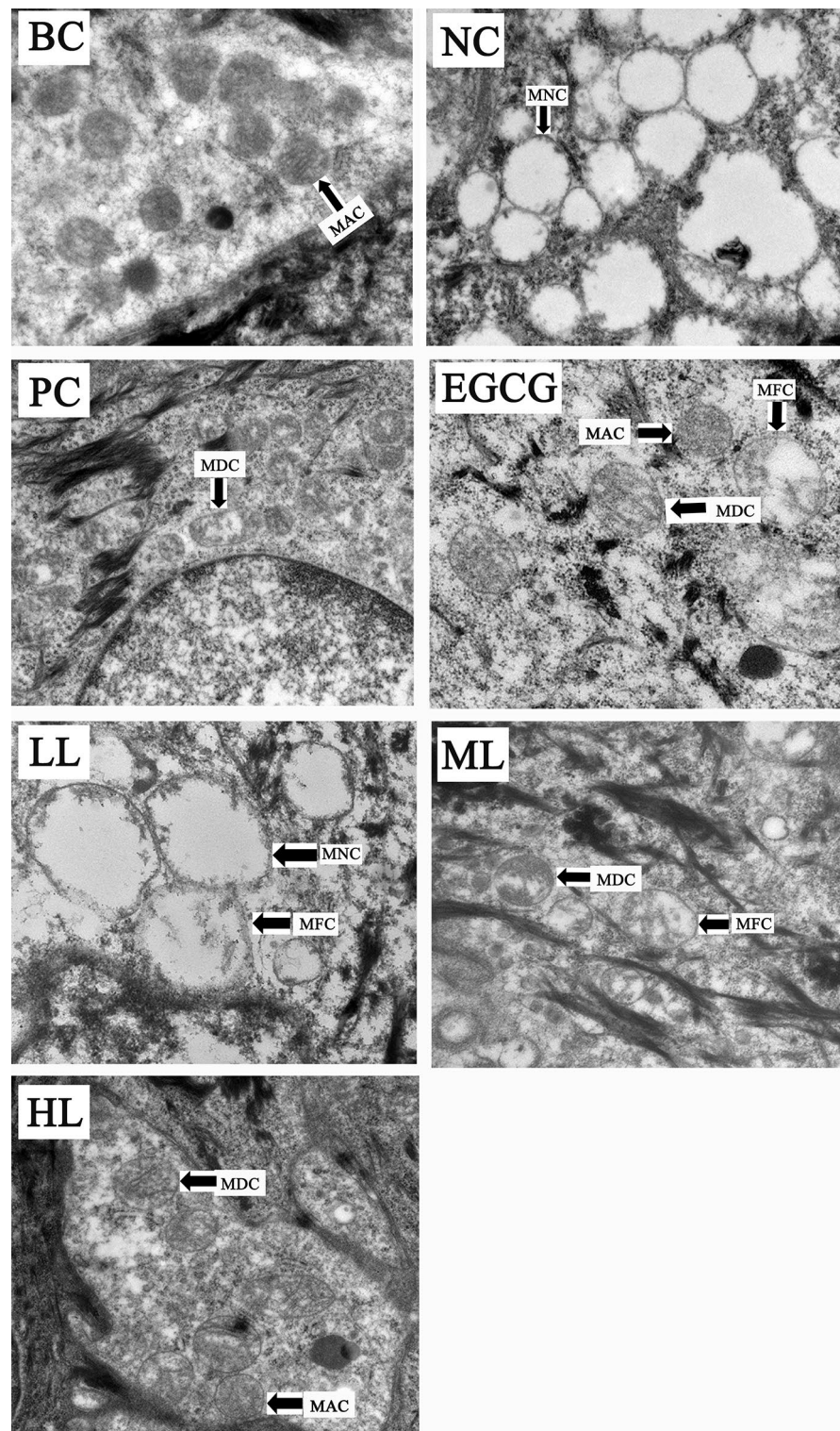


Figure 4. Effect of GCG on UVB-induced damage of mitochondria in skin of female hairless mice. *BC* blank control, *NC* negative control, *PC* positive control, *EGCG* EGCG treatment, *LL* low level GCG, *ML* medium level GCG, *HL* high level GCG, *MAC* mitochondrion with abundant cristae, *MDC* mitochondrion with decreased cristae, *MFC* mitochondrion with few cristae, *MNC* mitochondrion without cristae.

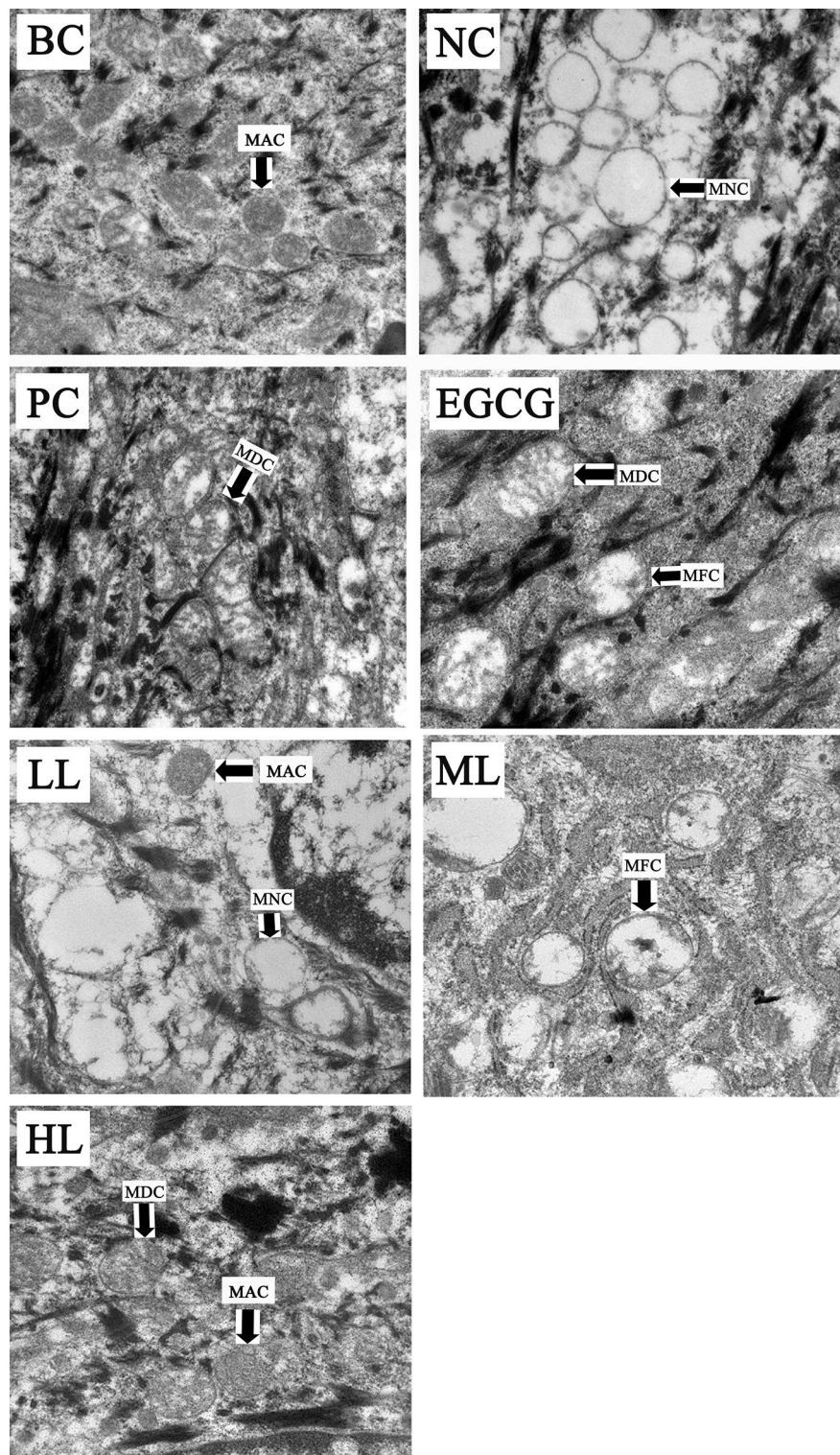


Figure 5. Effect of GCG on UVB-induced damage of mitochondria in skin of male hairless mice. *BC* blank control, *NC* negative control, *PC* positive control, *EGCG* EGCG treatment, *LL* low level GCG, *ML* medium level GCG, *HL* high level GCG, *MAC* mitochondrion with abundant cristae, *MDC* mitochondrion with decreased cristae, *MFC* mitochondrion with few cristae, *MNC* mitochondrion without cristae.

These suggest that GCG showed protective effects against mitochondria damages induced by UVB-irradiation in dose dependent manner.

Treatment	BC	NC	PC	EGCG	LL	ML	HL
Mitochondria injury index							
Male	0.07*	2.60 [§]	1.33 ^{§*}	1.53 ^{§*}	2.33 [§]	1.67 ^{§*}	1.40 ^{§*}
Female	0.20*	2.67 [§]	1.40 ^{§*}	1.60 ^{§*}	2.33 [§]	1.73 ^{§*}	1.40 ^{§*}

Table 3. Mitochondria damage index of various treatments. *Being significantly different from BC at $p < 0.05$. [§]Being significantly different from NC at $p < 0.05$.

Discussion

Skin photoaging is a complex process involving light stress like UVB. Healthy skin is biomechanically resilient, highly elastic, and characterized histologically by strong interdigitation of rete ridges, abundant organized fibrillar collagen, and plentiful arrays of elastic fibers²⁵. Skin elasticity depends on the condition of the extracellular matrix (ECM), which consists of primarily collagen. Collagen is an abundantly available protein structure in the ECM which is found in connective tissues of the human organs such as skin and is responsible for three-dimensional microstructure sustainability²⁶. There is a total of 28 different collagen types, in which type I (Col-I) is the most commonly found in the body²⁷. The Col-I monomers form triple-helical collagen structures through intertwining to form collagen fibrils, which are then assembled in bundles known as collagen fibers²⁸. Collagen provides mechanical support in many tissues of mammals and provides tensile strength in the skin through its widespread molecular line formation²⁹. Drugs with potential to improve collagen will be beneficial to skin health. Extract of *Foeniculum vulgare* (FV) significantly increased the production of collagen and elastin, showing dose-dependent decrease in production of reactive oxygen species (ROS) but increase in the expression of cytoprotective antioxidants such as glutathione, and significantly quenching UVB-induced phosphorylation of extracellular regulated protein kinases (ERK) and p38 mitogen-activated protein kinase (MAPK) in normal human skin fibroblasts³⁰. Polyphenols in combination with short exposure to UVA increased extracellular matrix deposition of elastin and collagen and improved skin properties^{31,32}. Present study shows that GCG, like EGCG, significantly suppressed the UVB-induced decrease in collagen fibers, compared to NC (Table 1), suggesting that GCG protected skin from UVB-induced photoaging via improving collagen functions.

Appropriate levels of skin moisture and skin lipid play a key role in the structure of stratum corneum and skin barrier function. Formulations containing marine sponge improved skin quality by increasing skin hydration and skin lipids³³. Hyaluronic acid, prolyl-hydroxyproline and hydroxyprolyl-glycine maintained skin moisture, resulting in improvement of skin conditions such as increase in elasticity and decrease in wrinkles and roughness^{34,35}. Ethanol extract of *Alchemilla mollis* effectively prevented UVB-induced skin water loss, resulting in alleviation of skin photoaging³⁶. The present study shows that the skin oil and moisture in NC and PC were significantly increased compared to BC (Table 1). However, these two indicators in ML and HL were lower than NC though they were higher than BC (Table 1), suggesting that GCG had no effects on prevention of skin oil and moisture loss. The human sebum, which is responsible for oily skin, is reported to exert a photoprotective effect and an increase in the sebum secretion contributed to an augmentation in the skin softness and elasticity^{32–34}. The oil levels in the UVB irradiated skins including those treated by sunscreen lotion and GCG were increased significantly (Table 1). These suggest the increase in skin oil level is a response of sebum to the UVB irradiation. However, the oil level in skin treated by EGCG was not significantly increased compared to BC though its skin elasticity was significantly higher than that in BC and NC (Table 1). Also, the skin elasticity in ML was significantly higher than those in NC and PC though its skin oil level was lower than the latter. These can be explained as: (1) EGCG and GCG at appropriate level partially absorbed the irradiated UVB where the sebum showed less response to the low level UVB. It is well known that catechins including EGCG and GCG have strong absorption around the wavelength of UVB. That is why the catechins are detected at 280 nm in quantitative studies. (2) The levels of collagen fibers in EGCG and ML were significantly higher than NC and LL, which might partially contribute to the skin elasticity.

In response to UVB irradiation, there was a marked increase in the number of melanosomes (Figs. 2 and 3), which was consistent with the previous study³⁷. The suppressive effects of GCG on melanosomes formation induced by UVB (Figs. 2 and 3, Table 2) explain why GCG treatment decreased the pigmentation (Table 1). Many studies show that inhibition of tyrosinase activity contributes to the suppression of skin pigmentation. Turmeric extract, salidroside and paeonol had potential for preventing pigmentation induced by UVB radiation via inhibiting the tyrosinase activity and melanin synthesis, and they were used as melanin formation inhibitors for hyperpigmentation therapy^{38,39}. Molecular docking showed that GCG and EGCG bound to the active center of tyrosinase and interacted with copper ions and key amino acid residues via hydrogen bonding and hydrophobic interactions, resulting in a looser conformation of tyrosinase and decrease in tyrosinase activity, during which the half maximal inhibitory concentration (IC_{50}) was $36.8 \pm 0.21 \mu\text{mol/L}$ for GCG and $39.4 \pm 0.54 \mu\text{mol/L}$ for EGCG^{40,41}. These suggest that GCG alleviated UVB-induced melanosome formation via suppressing tyrosinase activity.

The skin is a high turnover organ whose constant renewal depends on the rapid proliferation of its progenitor cells. The energy required for these metabolically active cells is supplied by mitochondrial respiration⁴² and so mitochondria play innate role in maintaining skin homeostasis and dysfunctions of mitochondria will lead to skin disorders. During mitochondrial respiration, reactive oxygen species (ROS) are inevitably produced, in which the ROS disrupts macromolecular and cellular structures if it is not quenched appropriately by the antioxidant system. The mitochondrial ROS-induced oxidative damage is the molecular basis for diverse pathophysiological issues including skin photoaging. Aberrations in the mitochondrial DNA (mtDNA) frequently take place in

photoaged skin lesions in which skin homeostasis and pigmentation are affected. The mitochondrial dysfunction is the direct consequence of UV-induced skin photoaging. Improving mitochondrial functions will be effective against skin photoaging and some skin diseases, and so therapeutic targeting in the skin, either via ATP production boost or free radical scavenging, has gained attention from clinicians⁴³. Mitochondrial membrane weakening triggers the autophagic process⁴⁴, which removes the damaged mitochondria induced by UVB irradiation. The mitophagy is one of the important repair mechanisms for UVB-induced damage⁴⁵. Anti-UVB agents such as nitrogen-phosphorous-doped carbon dots (NPCDs) induced the activation of autophagy by upregulating the protein expression levels of LC3-II and autophagy-related-5 (ATG-5)⁴⁶. EGCG protected skin against UVB induced photodamages by suppressing mitochondrial dysfunction⁴⁷. Glycyrrhizic acid significantly inhibited the UVB-induced skin photoaging via reducing ROS, NF- κ B, cytochrome C and caspase 3 levels⁴⁸. Present study shows that obvious aberrations were observed in mitochondria of NC and LL in which mitochondrial crest and matrix density were reduced, and vacuolation was increased. There were no significant differences in mitochondrial structures between treatments of ML, HL, BC and PC, in which mitochondrial membrane and mitochondrial matrix were clearly observed. These suggest that GCG protected skin photoaging by alleviating mitochondria dysfunction induced by UVB irradiation.

Bioavailability of tea catechins is an important factor influencing their pharmaceutical effects⁵⁰. EGCG uptake into and through mammalian skin is dependent on both the vehicle used and the length of topical exposure^{51,52}. Pure EGCG dissolved in acetone applied topically to mouse skin prevented UVB-induced photocarcinogenesis, whereas oral dosing is inactive^{51,53}. Nevertheless, meta-analysis showed that oral supplementation of green tea catechins complex was highly effective at low-intensity ultraviolet radiation-induced erythema response compared to placebo and regular supplementation of green tea catechins was associated with protection against UV-induced damage due to erythema inflammation^{54–57}. The absorption of EGCG dissolved in acetone into the mouse and human skins was more rapid than that in ointment formulation⁵². However, study also showed that human skin provides a much more efficient barrier than mouse skin for preventing systemic availability from topically applied EGCG⁵². Though GCG is confirmed to show a protective effect against UVB-induced mouse skin photodamages in the present study, researching an appropriate vehicle for GCG formula is still a topic in the future.

Conclusion

GCG protected hairless mice from UVB-induced skin photodamages by improving skin elasticity and collagen fibers, and inhibiting aberrations in mitochondria and formation of melanosomes. Because GCG is more chemically stable than its epimer counterpart EGCG⁴⁹ and it is not susceptible to environmental light, heat and oxygen, which endow it a good ingredient for sunscreen formula.

Received: 9 October 2021; Accepted: 10 January 2022

Published online: 25 January 2022

References

- Wang, P. W. *et al.* Comparison of the biological impact of UVA and UVB upon the skin with functional proteomics and immunohistochemistry. *Antioxidants* **8**, 569 (2019).
- Luo, D. & Zhou, B. R. Research progress on UV-induced skin damages and its prevention. *J. Dermatol. Venereol.* **31**, 18–20 (2009).
- Huang, J. *et al.* Asiatic acid glucosamine salt alleviates ultraviolet B-induced photoaging of human dermal fibroblasts and nude mouse skin. *Photochem. Photobiol.* **96**, 124–138 (2020).
- Bissett, D. L., Hannon, D. P. & Orr, T. V. Wavelength dependence of histological, physical, and visible changes in chronically UV-irradiated hairless mouse skin. *Photochem. Photobiol.* **50**, 763–769 (1989).
- Li, X. *et al.* Protective effects of astaxanthin supplementation against ultraviolet-induced photoaging in hairless mice. *Biomedicines* **8**, 18 (2020).
- Cichorek, M. *et al.* Skin melanocytes: Biology and development. *Postep. Dermatol. Alergol.* **30**, 30–41 (2013).
- Zhao, B. L. *et al.* UVB increases the expression of GPNMB and PMEL in sheep melanocytes. *Chin. J. Biochem. Mol. Biol.* **33**, 845–852 (2017).
- Addepalli, V. & Suryavanshi, S. V. Catechin attenuates diabetic autonomic neuropathy in streptozotocin induced diabetic rats. *Biomed. Pharmacother.* **108**, 1517–1523 (2018).
- Wang, S., Wu, S. & Liu, S. Integration of (+)-catechin and β -sitosterol to achieve excellent radical-scavenging activity in emulsions. *Food Chem.* **272**, 596–603 (2019).
- Liu, Y. X. *et al.* Therapeutic strategies of catechins for Alzheimer's disease aiming at amyloid cascade hypothesis. *J. Biol.* **33**(4), 73–77 (2016).
- Wu, M. Q. *et al.* Advances in bioavailability of catechins. *Sci. Technol. Food Ind.* **21**, 326–330 (2019).
- Li, X. Y. *et al.* Research progress on molecular mechanism of epigallocatechin-3-gallate against cancer and its application. *Zhong Cao Yao* **50**, 3217–3229 (2019) ((in Chinese)).
- Kofink, M., Papagiannopoulos, M. & Galensa, R. (-)-Catechin in cocoa and chocolate: Occurrence and analysis of an atypical flavan-3-ol enantiomer. *Molecules* **12**, 1274–1288 (2007).
- Ly, H. P. *et al.* Study on the GCG in green tea. *J. Tea Sci.* **28**(2), 79–82 (2008) ((in Chinese)).
- Yang, X. R. *et al.* Simultaneous analysis of purine alkaloids and catechins in *Camellia sinensis*, *Camellia ptilophylla* and *Camellia assamica* var. *Kucha* by HPLC. *Food Chem.* **100**, 1132–1136 (2007).
- Gao, X. *et al.* Cellular antioxidant, methylglyoxal trapping, and anti-inflammatory activities of cocoa tea (*Camellia ptilophylla* Chang). *Food Funct.* **8**, 2836–2846 (2017).
- Li, K. K. *et al.* Subacute oral toxicity of cocoa tea (*Camellia ptilophylla*) water extract in SD rats. *Int. J. Food Sci. Technol.* **50**, 2391–2401 (2015).
- Li, K. K. *et al.* Cocoa tea (*Camellia ptilophylla*) water extract inhibits adipocyte differentiation in mouse 3T3-L1 preadipocytes. *Sci. Rep.* **6**, 20172 (2016).
- Wu, L. Y., Zheng, X. Q., Lu, J. L. & Liang, Y. R. Protective effect of green tea polyphenols against ultraviolet B-induced damage to HaCaT cells. *Hum. Cell* **22**, 18–24 (2009).

20. Wang, C. P. *et al.* Density functional theory study on the antioxidant activity of EGCG and its stereoisomer GCG. *Nat. Prod. Res. Dev.* **27**, 645–650 (2015).
21. Wu, P. *Studied on the Thermal Stability of Epigallocatechin Gallate* 1–48 (Anhui Agricultural University, 2011).
22. Shen, S. R. Study on the scavenging effects of EGCG and GCG on singlet oxygen with ESR method. *J. Tea Sci.* **20**(1), 19–22 (2000) **(in Chinese)**.
23. Guo, Q. ESR study on the structure-antioxidant activity relationship of tea catechins and their epimers. *Biochim. Biophys. Acta* **1427**, 13–23 (1999).
24. Mouls, L. & Fulcrand, H. Identification of new oxidation markers of grape-condensed tannins by UPLC-MS analysis after chemical depolymerization. *Tetrahedron* **71**, 3012–3019 (2015).
25. Langton, A. K. Aging in skin of color: Disruption to elastic fiber organization is detrimental to skin's biomechanical function. *J. Invest. Dermatol.* **139**, 779–788 (2019).
26. Milazzo, M. Wave propagation and energy dissipation in collagen molecules. *ACS Biomater. Sci. Eng.* **6**, 1367–1374 (2020).
27. Jung, G. S. & Buehler, M. J. Multiscale modeling of muscular-skeletal systems. *Annu. Rev. Biomed. Eng.* **19**, 435–457 (2017).
28. Radhakrishnan, S. *et al.* Collagen based biomaterials for tissue engineering applications: A review. In *Lecture Notes in Earth System Sciences* (eds Frank-Kamenetskaya, O. V. *et al.*) 3–22 (Springer, 2020).
29. Lo, S. & Fauzi, M. B. Current update of collagen nanomaterials—fabrication, characterisation and its applications: A review. *Pharmaceutics* **13**, 316 (2021).
30. Sun, Z. *et al.* Dietary *Foeniculum vulgare* Mill extract attenuated UVB irradiation-induced skin photoaging by activating of Nrf2 and inhibiting MAPK pathways. *Phytomedicine* **23**, 1273–1284 (2016).
31. Sandilands, A. *et al.* Filaggrin in the frontline: Role in skin barrier function and disease. *J. Cell Sci.* **122**, 1285–1294 (2009).
32. Chowdhury, A. *et al.* Polyphenol treatments increase elastin and collagen deposition by human dermal fibroblasts; Implications to improve skin health. *J. Dermatol. Sci.* **102**, 94–100 (2021).
33. Swatschek, D. *et al.* Marine sponge collagen: isolation, characterization and effects on the skin parameters surface-pH, moisture and sebum. *Eur. J. Pharm. Biopharm.* **53**, 107–113 (2002).
34. Wiest, L. & Kersch, M. Native hyaluronic acid in dermatology-Results of an expert meeting. *J. Dtsch. Dermatol. Ges.* **6**, 176–180 (2008).
35. Inoue, N., Sugihara, F. & Wang, X. Ingestion of bioactive collagen hydrolysates enhance facial skin moisture and elasticity and reduce facial ageing signs in a randomised double-blind placebo-controlled clinical study. *J. Sci. Food Agric.* **96**, 4077–4081 (2016).
36. Hwang, E. *et al.* Protective effect of dietary *Alchemilla mollis* on UVB-irradiated premature skin aging through regulation of transcription factor NFATc1 and Nrf2/ARE pathways. *Phytomedicine* **39**, 125–136 (2018).
37. Ichihashi, M. *et al.* UV-induced skin damage. *Toxicology* **189**, 21–39 (2003).
38. Peng, L. H. *et al.* Inhibitory effects of salidroside and paeonol on tyrosinase activity and melanin synthesis in mouse B16F10 melanoma cells and ultraviolet B-induced pigmentation in guinea pig skin. *Phytomedicine* **20**, 1082–1087 (2013).
39. Sumiyoshi, M. & Kimura, Y. Effects of a turmeric extract (*Curcuma longa*) on chronic ultraviolet B irradiation-induced skin damage in melanin-possessing hairless mice. *Phytomedicine* **16**, 1137–1143 (2009).
40. Song, X. *et al.* Comparing the inhibitory abilities of epigallocatechin-3-gallate and gallic acid against tyrosinase and their combined effects with kojic acid. *Food Chem.* **349**, 129172 (2021).
41. Lee, X. Z. *et al.* Alleviation of UV-B stress in *Arabidopsis* using tea catechins. *Afr. J. Biotechnol.* **7**, 4111–4115 (2008).
42. Hatefi, Y. The mitochondrial electron-transport and oxidative-phosphorylation system. *Annu. Rev. Biochem.* **54**, 1015–1069 (1985).
43. Sreedhar, A., Aguilera-Aguirre, L. & Singh, K. K. Mitochondria in skin health, aging, and disease. *Cell Death Dis.* **11**, 444 (2020).
44. Chen, Z. Y., Liu, X. D. & Ma, S. M. The roles of mitochondria in autophagic cell death. *Cancer Biother. Radiopharm.* **31**, 269–276 (2016).
45. Dundar, G., Teranishi, M. & Hidema, J. Autophagy-deficient *Arabidopsis* mutant atg5, which shows ultraviolet-B sensitivity, cannot remove ultraviolet-B-induced fragmented mitochondria. *Photochem. Photobiol. Sci.* **19**, 1717–1729 (2020).
46. Bajpai, V. K. *et al.* Multifunctional N-P-doped carbon dots for regulation of apoptosis and autophagy in B16F10 melanoma cancer cells and in vitro imaging applications. *Theranostics* **10**, 7841–7856 (2020).
47. Liu, C. *et al.* Protective effect of (-)-epigallocatechin gallate on ultraviolet b-induced skin damage in hairless mice. *Trop. J. Pharm. Res.* **15**, 1183–1189 (2016).
48. Afnan, Q. *et al.* Glycyrrhizic acid (GA), a triterpenoid saponin glycoside alleviates ultraviolet-B irradiation-induced photoaging in human dermal fibroblasts. *Phytomedicine* **19**, 658–664 (2012).
49. Xie, L. W. *et al.* Epimerization of epigallocatechin gallate to gallic acid and its anti-diabetic activity. *Med. Chem. Res.* **22**, 3372–3378 (2013).
50. Cai, Z. Y. *et al.* Bioavailability of tea catechins and its improvement. *Molecules* **23**, 2346 (2018).
51. Gensler, H. L. *et al.* Prevention of photocarcinogenesis by topical administration of pure epigallocatechin gallate isolated from green tea. *Nutr. Cancer* **26**, 325 (1996).
52. Dvorakova, K. *et al.* Pharmacokinetics of the green tea derivative, EGCG, by the topical route of administration in mouse and human skin. *Cancer Chemoth. Pharm.* **43**, 331–335 (1999).
53. Farrar, M. D. Oral green tea catechins do not provide photoprotection from direct DNA damage induced by higher dose solar simulated radiation: A randomized controlled trial. *J. Am. Acad. Dermatol.* **78**, 414–416 (2018).
54. Farrar, M. D. *et al.* A randomized controlled trial of green tea catechins in protection against ultraviolet radiation-induced cutaneous inflammation. *Am. J. Clin. Nutr.* **102**, 608–615 (2015).
55. Rhodes, L. E. *et al.* Oral green tea catechin metabolites are incorporated into human skin and protect against UV radiation-induced cutaneous inflammation in association with reduced production of pro-inflammatory eicosanoid 12-hydroxyeicosatetraenoic acid. *Br. J. Nutr.* **110**, 891–900 (2013).
56. Heinrich, U., Moore, C. E., De Spirt, S., Tronnier, H. & Stahl, W. Green tea polyphenols provide photoprotection, increase microcirculation, and modulate skin properties of women. *J. Nutr.* **141**, 1202–1208 (2011).
57. Kapoor, M. P. *et al.* Green tea catechin association with ultraviolet radiation-induced erythema: A systematic review and meta-analysis. *Molecules* **26**, 3702 (2021).

Acknowledgements

The authors appreciated the Chun'an Economic Development Zone management Committee, the Ministry of Finance (MOF) and the Ministry of Agriculture and Rural Affairs (MARA) for financial support to the present study.

Author contributions

Y.R.L., X.Q.Z. & Z.J.C., conceived the project and prepared the manuscript draft. Y.Y.S., J.X., J.L.L., J.H.Y., J.W.Z., Y.R.L. & X.Q.Z., performed experiments and prepared draft figures and tables, prepared the manuscript draft. All authors approved the final manuscript.

Funding

This research was financially supported by Chun'an Economic Development Zone management Committee and the China Agriculture Research System of MOF and MARA.

Competing interests

The authors declare no competing interests.

Additional information

Supplementary Information The online version contains supplementary material available at <https://doi.org/10.1038/s41598-022-05305-9>.

Correspondence and requests for materials should be addressed to Y.-R.L. or X.-Q.Z.

Reprints and permissions information is available at www.nature.com/reprints.

Publisher's note Springer Nature remains neutral with regard to jurisdictional claims in published maps and institutional affiliations.



Open Access This article is licensed under a Creative Commons Attribution 4.0 International License, which permits use, sharing, adaptation, distribution and reproduction in any medium or format, as long as you give appropriate credit to the original author(s) and the source, provide a link to the Creative Commons licence, and indicate if changes were made. The images or other third party material in this article are included in the article's Creative Commons licence, unless indicated otherwise in a credit line to the material. If material is not included in the article's Creative Commons licence and your intended use is not permitted by statutory regulation or exceeds the permitted use, you will need to obtain permission directly from the copyright holder. To view a copy of this licence, visit <http://creativecommons.org/licenses/by/4.0/>.

© The Author(s) 2022